Synthesis, crystal structure and physical properties of $NaMnFe(MoO_4)_3$

Manel Mhiri [a], Abdessalem Badri[a], Maria Luisa Lopez[b], Carlos Pico [b], Mongi Ben Amara [a*]

[a] *UR : Matériaux Inorganiques, Faculté des Sciences, Université de Monastir, 5019 Monastir, Tunisie.*
[b] *Departamento de Quimica Inorganica I. Facultad de Ciencias Quimicas, Universidad Complutense, 28040 Madrid, Spain.*

(Received: 26 June 2016, accepted: 07 November 2016)

Abstract: Iron molybdate $NaMnFe(MoO_4)_3$ has been synthesized by flux method and solid state reaction, and characterized by X-ray diffraction, magnetic susceptibility and ionic conductivity. This compound is isostructural with α-$NaFe_2(MoO_4)_3$ and crystallizes in the triclinic space group $P\bar{1}$ with the cell parameters: a = 6.963(3) Å, b = 6.998(1) Å, c = 11.169(2) Å, α = 79.88(1)°, β = 84.01(3)°, γ = 80.81(3)° and Z = 2. Its structure is built up from $[Mn,Fe]_2O_{10}$ units of edge-sharing $[Mn,Fe]O_6$ octahedra which are linked to each other through the common corners of MoO_4 tetrahedra. The resulting anionic three-dimensional framework leads to the formation of channels along the [101] direction, where the Na^+ cations are located. The disordered distribution of iron and manganese in the same site is confirmed by bond valence calculation. Magnetic measurements show that this compound to be antiferromagnetic with C_m = 9.03 emu K/mol and θ = -65.5 K. Ionic conductivity results of the title compound reveal an activation energy E_a = 0.95 eV noticeably higher than E_a< 0.36 eV observed for $NaMFe(MoO_4)_3$ (M = Ni, Zn) . This disparity can be related to the difference between the structural characteristics of both kinds of compounds.

Keywords: Iron molybdate; X-ray diffraction; Magnetic measurements; Ionic conductivity.

INTRODUCTION

Iron molybdates are subject to very intensive research for many applications. For example, Simple molybdate $Fe_2(MoO_4)_3$ is very promising for catalysis [1,2], the double molybdates $MFe(MoO_4)_2$ (M=Na, K, Rb) exhibit interesting multiferroic properties [3-5] and $LiFe(MoO_4)_2$ is considered as a possible positive electrode in rechargeable batteries [6]. In these materials, the anionic framework is constructed from MoO_4 tetrahedra linked to the iron coordination polyhedra leading to a large variety of crystal structures with a high capacity for cationic and anionic substitutions. This versatility is essentially due to the double ability of iron to adopt a mixed valence and various coordination polyhedra $[FeO]_n$ with n = 4, 5 and 6.

Until now a total of six orthomolybdate compounds have been reported in the Na–Fe–Mo–O system [7-10]: $Na_9Fe(MoO_4)_6$, $NaFe(MoO_4)_2$, α-$NaFe_2(MoO_4)_3$, β-$NaFe_2(MoO_4)_3$, $Na_3Fe_2(MoO_4)_3$ and $NaFe_4(MoO_4)_5$. Their structures are described in term of three-dimensional networks of isolated $[MoO_4]$ tetrahedra and $[FeO_6]$ octahedra. The sodium and mixed valence iron molybdate $NaFe_2(MoO_4)_3$ exhibits two polymorphs, both crystallizing in the triclinic system. The low-temperature α-phase changes irreversibly at high-temperature into a β-phase. In addition to these orthomolybdate compounds, another phase with the formula $Na_3Fe_2Mo_5O_{16}$ and with layers of Mo_3O_{13} clusters consisting of $[MoO_6]$ octahedra was synthesized and characterized [11].

Recently, N. M. Kozhevnikova et al. have investigated the Na_2MoO_4-$MMoO_4$-$Fe_2(MoO_4)_3$ system (M = Mg, Mn, Ni, Co) and have attributed to the phase of variable composition $Na_{(1-x)}M_{(1-x)}Fe_{(1+x)}(MoO_4)_3$ the type-NASICON structure with space group $R\bar{3}c$ [12, 13]. More recently $NaNiFe(MoO_4)_3$ and $NaZnFe(MoO_4)_3$[14] were found isostructural to β-$NaFe_2(MoO_4)_3$ and having a good ionic conductivity with low activation energy close to

* Corresponding author, e-mail address : mongi.benamara@fsm.rnu.tn

those of Nasicon-type compounds with similar formula such as $AZr_2(PO_4)_3$ (A = Na, Li).

As an extension of the previous works, we report here on the synthesis and characterization by X-ray diffraction, magnetic susceptibility and ionic conductivity of a new compound $NaMnFe(MoO_4)_3$ isostructural with α-$NaFe_2(MoO_4)_3$.

EXPERIMENTAL

1. Synthesis

Crystals of the title compound were grown in a flux of sodium dimolybdate $Na_2Mo_2O_7$ with an atomic ratio Na:Mn:Fe:Mo = 5:1:1:7. Appropriate amounts of starting reactants $NaNO_3$, $Mn(NO_3)_2.6H_2O$, $Fe(NO_3)_3.9H_2O$ and $(NH_4)_6Mo_7O_{24}.4H_2O$ were dissolved in nitric acid and the resulting solution was evaporated to dryness. The dry residue was then placed in a platinum crucible and slowly heated in air up to 673K for 24 h to remove H_2O and NH_3. The mixture was ground in an agate mortar, melted for 2 h at 1123K and then cooled to room temperature at 5 Kh^{-1} rate. Crystals without regular shape were separated from flux by washing in boiling water.

After the structural determination, a polycrystalline sample was synthesized by soft combustion synthesis technique [15] according to the following procedure. First, stoichiometric amounts of $NaNO_3$, $Mn(NO_3)_2.6H_2O$, $Fe(NO_3)_3.9H_2O$ and $(NH_4)_6Mo_7O_{24}.4H_2O$ were dissolved in distilled water, then mixed with aqueous glycine solution. The stoichiometric composition of glycine was taken to be twice the molar fraction of the starting materials. The obtained brown solution is heated to boiling at about 373 K leading to the formation of dark-brown paste-like substance which is subsequently heated for 6h at 523 K. The final step in this procedure is the calcination of the formed dark-brown powder for 24 h in air at 943 K. The purity of the synthesized powder was checked by the examination of its X-ray diagram collected in the range 5° ≤ 2θ ≤ 100° on a PANalytical diffractometer using CuK_α radiation (λ=1.5406Å).

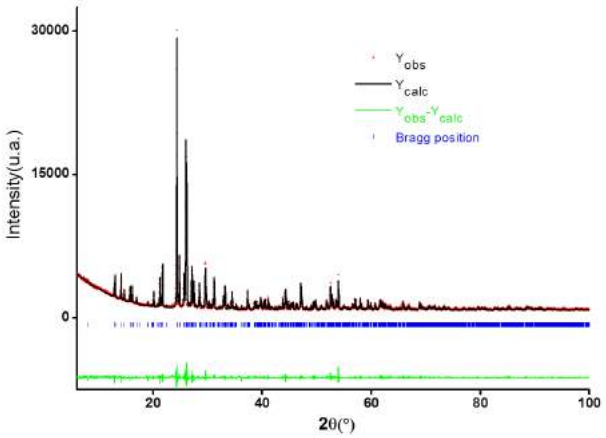

Figure 1: Powder X-ray patterns for $NaMnFe(MoO_4)_3$

The X-ray powder patterns reported in Figure 1 indicate that $NaMnFe(MoO_4)_3$ is isostructural with α-$NaFe_2(MoO_4)_3$ [9]. No additional peaks due to any impurity phase were observed at the resolution limit of the instrument. The refined cell parameters are reported in Table I.

2. Structure determination

The structure of $NaMnFe(MoO_4)_3$ was determined from single crystal X-ray diffraction data, collected at room temperature by an Enraf-Nonius CAD4 diffractometer using graphite monochromated MoK_α radiation (λ = 0.7107 Å). The unit cell parameters and the orientation matrix were determined from a least-squares fit of 25 reflections in the range 9.11° ≤ θ ≤ 14.47°. A total of 3062 unique reflections measured with a maximum 2θ of 60° for the (±h, ±k,l) hemisphere (R_{in} = 0.016) but only 2721 were considered as observed according to the statistic criterion [I>2σ(I)]. The measured intensities were corrected for Lorentz and polarisation effects. Then, an empirical absorption correction was performed using Psi-scan method [16]. Relevant

Table I : Cell parameters of $NaMnFe(MoO_4)_3$ compared to those of α-$NaFe_2(MoO_4)_3$[12].

	a (Å) / α(°)	b (Å) / β(°)	c (Å) / γ(°)	V ($Å^3$)	Ref.
$NaMnFe(MoO_4)_3$	6.963 (3) 79.88 (1)	6.998 (1) 84.01 (3)	11.169 (2) 80.81 (3)	527.3 (3)	This work
α-$NaFe_2(MoO_4)_3$	6.9253 (4) 80.205 (6)	6.9513 (4) 83.679 (6)	11.0600 (9) 80.818 (5)	516.06(6)	[9]

Table II: Details of the data collection and structural refinement for $NaMnFe(MoO_4)_3$.

Crystal data	
Chemical formula	$NaMnFe(MoO_4)_3$
Formula weight (g/mol)	613.60
Crystal system	Triclinic
Space group	$P\bar{1}$
a (Å) / α (°)	6.963(3) / 79.88(1)
b (Å) / β (°)	6.998(1) / 84.01(3)
c (Å) / γ (°)	11.169(2) / 80.81(3)
Volume ($Å^3$) / Z	527.3 (3) / 2
ρ_{cal} (Kg/m^3)	3.865×10^3
Intensity measurements	
Crystal dimensions (mm^3)	0.04 × 0.11× 0.21
Apparatus	CAD4 (Enraf-Nonius)
$\lambda_{Mo}K\alpha$ (Å)	0.71073
Monochromator	Graphite
μ (mm^{-1})	6.075
Scan mode	ω/2θ
θ range	2,97 ≤θ≤ 29,96
Unique reflections; R_{int}	3062; 0.016
Observed reflections (I> 2σ(I))	2721
Indices	$-9 \le h \le 9$; $-9 \le k \le 9$; $-1 \le l \le 15$
F (000)	568
Structure solution and refinement	
Intensity correction	Lorentz-Polarization
Absorption correction	Psi-scan
$T_{min\ ;\ max}$	0.646 ; 0.781
Resolution method	Direct method
Agreement factors	R_1=0.032; $wR_2(F^2)$ =0.081; S = 1.06 (I > 2σ(I))
Number of refined parameters	164
Extinction coefficient	0.0065(7)
Weighting scheme	$W = 1/[\sigma^2(F_o^2)+(0.0525P)^2+1.0601P]$ where $P = (F_o^2+2F_c^2)/3$
$(\Delta\rho)_{max;min}$ (e. $Å^{-3}$)	1.786; -2.154

Table III: Fractional atomic coordinates and equivalent isotropic displacement parameters ($Å^2$) for $NaMnFe(MoO_4)_3$.

Site	Atom	x()	y()	z()	U_{eq}() *
Na	Na	0.8458(4)	0.5813(4)	0.8408(4)	0.0721(13)
[Mn,Fe](1)	0.5Mn+0.5Fe	0.81118(8)	0.17093(8)	0.50874(5)	0.01042(13)
[Mn,Fe](2)	0.5Mn+0.5Fe	0.77253(8)	0.77755(8)	0.11355(5)	0.00887(13)
Mo(1)	Mo	0.75835(5)	0.09882(5)	0.85038(3	0.01005(10)
O(11)	O	0.8145(4)	0.8534(4)	0.9291(3)	0.0147(6)
O(12)	O	0.9313(4)	0.2509(4)	0.8697(3)	0.0171(6)
O(13)	O	0.5198(5)	0.2051(5)	0.8919(3)	0.0197(6)
O(14)	O	0.7733(6)	0.0817(5)	0.6971(3)	0.0237(7)
Mo(2)	Mo	0.70534(5)	0.28488(5)	0.18685(3)	0.01174(10)
O(21)	O	0.4607(5)	0.3462(5)	0.2246(3)	0.0256(7)
O(22)	O	0.7419(5)	0.0716(5)	0.1166(4)	0.0250(7)
O(23)	O	0.8348(5)	0.2342(5)	0.3186(3)	0.0230(7)
O(24)	O	0.8009(5)	0.4885(5)	0.0916(3)	0.0181(6)
Mo(3)	Mo	0.27227(5)	0.29876(5)	0.54437(3)	0.01015(10)
O(31)	O	0.1207(4)	0.1348(4)	0.5073(3)	0.0157(6)
O(32)	O	0.2497(5)	0.3011(5)	0.7017(3)	0.0234(7)
O(33)	O	0.5130(5)	0.2116(6)	0.5026(3)	0.0246(7)
O(34)	O	0.2070(5)	0.5369(5)	0.4659(3)	0.0232(7)

crystallographic data and structure refinements details are summarized in Table II.

The structure was solved in the triclinic space group $P\bar{1}$ by direct methods using the SIR-92 program [17] which revealed the positions of molybdenum atoms. The remaining atoms were located by Fourier synthesis alternating with least-squares structure refinement based on F^2 (SHELXL-97) [18]. A possible disordered distribution of Fe^{3+} and Mn^{2+} in the same crystallographic sites was considered due to their similar ionic radii ($r(Fe^{3+})$ = 0.645Å; $r(Mn^{2+})$ = 0.67 Å [19]. The refinements based on this hypothesis converged to a distribution close to: 0.5 Fe + 0.5 Mn. The occupancy factors of atoms of Fe and Mn in both sites were then fixed to the value 0.5. The final cycle of refinement, including the anisotropic thermal parameters for all atoms, converged at R_1 = 0.032 and $wR_2(F^2)$ = 0.081 for the observed reflections, which confirms consequently the proposed formula. Fractional atomic coordinates and isotropic thermal parameters are given in Table III and selected bond distances in Table IV. All calculations were performed using the Wingx software package [20].

Further details of the crystal structure determination can be ordered from Fachinformationszentrum Karlsruhe, 76344 Eggenstein-Leopoldshafen, under the depository number CSD 431120.

In order to confirm the proposed cationic distribution, the final structural model was examined with bond valence sum (BVS) calculations using Chardi (CD) method [21]. The charge distribution was calculated using the CHARDI-IT program [22] leading to the results reported in Table 5. This method is used to validate structures, as in the case where some atoms are disordered in the same crystallographic site [23]. In the present structure, the calculated valences of all the sites are consistent with their formal charges. In particular, the valence close to 2.50 calculated

Table IV: Selected interatomic distances (Å) in the coordination polyhedra of $NaMnFe(MoO_4)_3$.

	$[M,Fe]O_6$ octahedra			NaO_8 polyhedron	
[Mn,Fe](1)-O(33)	2.057(3)	[Mn,Fe](2)-O(13)	2.026(3)	Na-O(11)	2.265(4)
[Mn,Fe](1)-O(23)	2.086(4)	[Mn,Fe](2)-O(32)	2.036(3)	Na-O(12)	2.268(4)
[Mn,Fe](1)-O(14)	2.088(3)	[Mn,Fe](2)-O(11)	2.038(3)	Na-O(21)	2.279(4)
[Mn,Fe](1)-O(34)	2.095(3)	[Mn,Fe](2)-O(22)	2.041(3)	Na-O(31)	2.545(9)
[Mn,Fe](1)-O(31)	2.129(3)	[Mn,Fe](2)-O(24)	2.056(3)	Na-O(32)	2.830(9)
[Mn,Fe](1)-O'(31)	2.151(3)	[Mn,Fe](2)-O(12)	2.065(3)	Na-O(24)	2.595(4)
				Na-O'(24)	2.759(6)
				Na-O(23)	3.011(5)
	MoO_4 tetrahedra				
Mo(1)-O(14)	1.729(3)	Mo(2)-O(21)	1.716(4)	Mo(3)-O(33)	1.735(3)
Mo(1)-O(13)	1.759(3)	Mo(2)-O(23)	1.759(3)	Mo(3)-O(32)	1.750(3)
Mo(1)-O(12)	1.781(3)	Mo(2)-O(22)	1.777(3)	Mo(3)-O(34)	1.755(3)
Mo(1)-O(11)	1.789(3)	Mo(2)-O(24)	1.797(3)	Mo(3)-O(31)	1.802(3)

Table V: Charge distribution (CD) sum calculation of $NaMnFe(MoO_4)_3$.

Cation	Q_i	q_i	Anion	Q_i	q_i
Na	0.984	1	O11	-2.085	-2.000
[Mn,Fe](1)	2.463	2.5	O12	-2.090	-2.000
[Mn,Fe](2)	2.543	2.5	O13	-1.967	-2.000
Mo(1)	5.815	6	O 14	-2.118	-2.000
Mo(2)	6.236	6	O21	-2.019	-2.000
			O22	-1.844	-2.000
			O23	-1.953	-2.000
			O24	-1.864	-2.000
Mo(3)	5.958	6	O31	-2.031	-2.000
			O32	-1.976	-2.000
			O33	-2.102	-2.000
			O34	-1.951	-2.000
σ = 0.138				σ = 0.091	

Qi: computed charge; *qi*: formal oxidation number;

Charge dispersion: $\sigma = \sum_{i=1}^{n}[(q_i - Q_i)^2 / N - 1]^{1/2}$

for [Mn,Fe](1)O_6 and [Mn,Fe](2)O_6 sites are in good agreement with that predicted by the structural refinement.

3. Characterization

The magnetic susceptibility measurements were carried out in the 2-300 K temperature range, under a constant applied field of 500 Oe by a Quantum Design SQUID magnetometer.

Electrical properties have been performed from the analysis of ac complex impedance spectroscopy. A Solartron SI 1260 impedance/gain -phase Analyser was used with frequencies ranging from 1 Hz to 10 MHz in the temperature regions 473-633K. Cylindrical pellets were prepared by compressing the powder (5 ton) to 1.32 mm in height and 13 mm in diameter, sintered at 943 K during 48 h and coated with platinum paint on both sides. X-ray patterns showed that no phase changes took place. The absence of water in the initial and final samples was confirmed by IR spectra, excluding therefore any possible contribution of protonic conductivity in these processes. Measurements were carried out in nitrogen atmosphere, increasing the temperature at a rate of 1 $K.min^{-1}$ and stabilizing the temperature before collecting data.

RESULTS AND DISCUSSION

1. Description of the structure

The $NaMnFe(MoO_4)_3$ structure is based on a three-dimensional framework of $[Mn,Fe]_2O_{10}$ units of edge-sharing [Mn,Fe]O_6 octahedra, connected to each other through the common corners of MoO_4 tetrahedra. All $[Mn,Fe]_2O_{10}$ units are parallel to the direction [1 $\bar{1}$ 0] (Fig. 2).In this structure, two types of layers (A) and (B) similar to those observed in α-$NaFe_2(MoO_4)_3$ are stacked parallel to the (**a**, **b**) plane with the sequence -A-B-B'-A-B-B'- along the **c** direction. Layers (B') are obtained from (B) by an inversion symmetry located on the (A) planes (Fig. 3). The resulting anionic three-dimensional framework leads to the formation of channels along the [1 0 1] direction, where the sodium ions are located (Fig. 4).

In this structure, all atoms are located in general positions. The three crystal-lographically different molybdenum atoms have a tetrahedral coordination with Mo–O distances included between 1.708(5) Å and 1.832(4) Å. Their mean distances<Mo(1)–O> = 1.765 Å, <Mo(2)–O> = 1.762 Å and <Mo(3)–O>

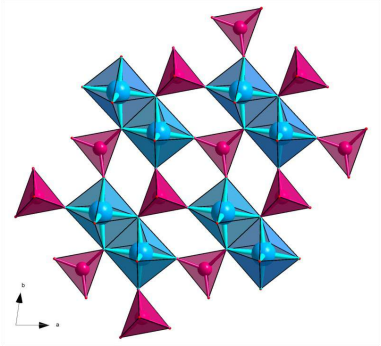

Figure 2: $[Mn,Fe]_2O_{10}$ units parallel to the direction [1 $\bar{1}$ 0] in $NaMnFe(MoO_4)_3$ structure.
Legend: $[Mn,Fe]_2O_{10}$ dimers = blue and MoO_4 tetrahedra = purple.

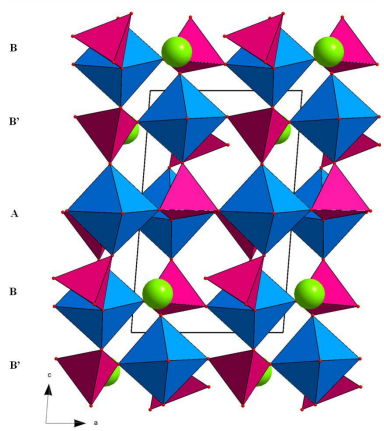

Figure 3: Projection of the $NaMnFe(MoO_4)_3$ structure along the **b** axis.
Legend: $[Mn,Fe]_2O_{10}$ dimers = blue; MoO_4 tetrahedra = purple and Na^+ cations = green circles.

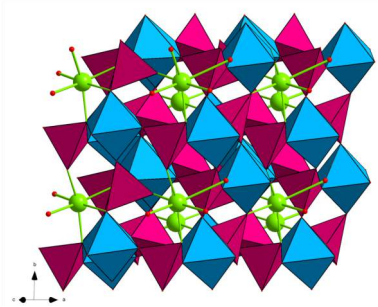

Figure 4: Channels along the [1 0 1] direction in the $NaMnFe(MoO_4)_3$.
Legend: $[Mn,Fe]_2O_{10}$ dimers = blue; MoO_4 tetrahedra = purple and Na^+ cations = green circles.

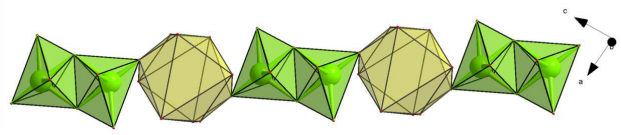

Figure 5: Na_2O_{14} dimers alternating cento-symmetric interstitial spaces at Wyckoff position: ***1a*** in $NaMnFe(MoO_4)_3$ structure.

= 1.761 Å are in a good accordance with those usually observed in molybdates [24-26].

The [Mn,Fe]–O distances and the cis O–[Mn,Fe]–O angles in the $[Mn,Fe]_2O_{10}$ unit range from 2.026(3) Å to 2.151(3) Å and from 80.2(1)° to 100.4(1)° respectively. This dispersion reflects a slight distortion of $[Mn,Fe]O_6$ octahedra. The average distances <[Mn,Fe](1)–O> = 2.101 Å and <[Mn,Fe](2)–O> = 2.044 Å are between 1.990 Å observed for six-coordinated Fe^{3+} in $LiFe(MoO_4)_2$ [27] and 2.138 Å reported for Mn^{2+} with the same coordination in $Rb_2Mn_2(MoO_4)_3$ [28]. This result is related to the disordered distribution of Fe^{3+} and Mn^{2+} in both sites.

Assuming sodium-oxygen distances below 3.13 Å as suggested by Donnay and Allmann [29], the Na site is surrounded by eight oxygen atoms. Two NaO_8 polyhedra related by an inversion centre are sharing edge and form a Na_2O_{14} dimer. In the [1 0 1] direction, the tunnel can be considered as made up of Na_2O_{14} dimers alternating cento-symmetric interstitial spaces at Wyckoff position: ***1a*** (Fig.5). As a consequence, the motion of sodium cations through the tunnels seems feasible. This possibility will be confirmed by the electrical measurements.

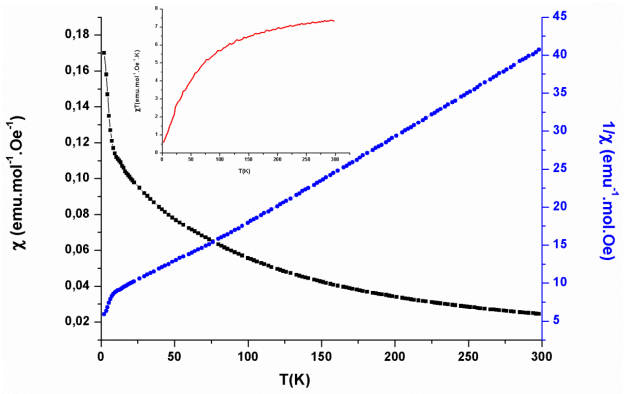

Figure 6: Magnetic and the reciprocal susceptibilities versus temperature for $NaMnFe(MoO_4)_3$.

2. Magnetic behavior

In order to assess possible cooperative interactions between the paramagnetic cations of the $[Mn,Fe]_2O_{10}$ structural units, the thermal variations of the magnetic susceptibility and its reciprocal for $NaMnFe(MoO_4)_3$ are shown in Figure 6. In the 2-300 K temperature range, the evolution of χvs temperature clearly follows a Curie-Weiss law, $\chi = C/(T - \theta)$. The experimental Curie constant, C = 9.03 emu mol^{-1} K, and effective magnetic moment, μ = 8.5 μ_B, are in accordance with the theoretical values, taking into account the spin contribution for the Mn^{2+} and Fe^{3+} magnetic cations: C = 8.76 emu mol^{-1} K and

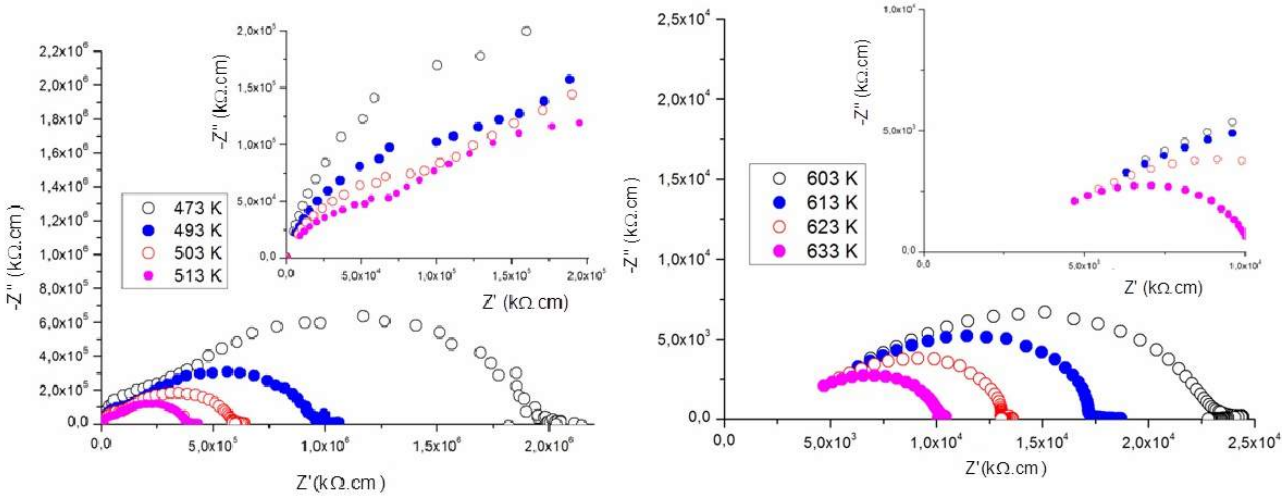

Figure 7: Cole-Cole plot at different temperatures for $NaMnFe(MoO_4)_3$.

μ = 8.37 μ_B. Otherwise, the alternative distribution of oxidation states, Mn^{2+} and Fe^{3+}, that also agrees with the mean values, q_i = 2.5 (Table V), gives rise to a Curie-Weiss constant, C = 6.0 emu mol^{-1} K, that is very different from the experimental value. On the other hand, the Weiss temperature determined through a linear least squares extrapolation to zero has negative value θ = -65.5 K, suggesting therefore that antiferromagnetic interactions appear at very low temperatures. Nevertheless, no minima are found in the magnetic susceptibility variations for $NaMnFe(MoO_4)_3$ down to 4 K, although the above interactions are suggested from the deviations found in the reciprocal susceptibility graph. This assumption is also in agreement with the very low value of $\chi \cdot T$ obtained at low temperatures, as shown in the inset of Figure 6. The suggested interactions are weak and no additional measurements were carried out.

3. Ionic conductivity

The electrical behaviour of the $NaMnFe(MoO_4)_3$ was studied over a wide range of frequency and temperature using a.c. technique of complex impedance spectroscopy. Figure 7 shows the complex impedance diagrams (imaginary part of complex impedance vs. real part, Nyquist plots) measured at different temperatures. In the temperature interval 473-513 K, an incipient arc and a second well resolved arc spanning the whole frequency range are obtained. The arcs take the shape of semicircle at higher temperature and the radius decreases as temperature rises, which indicates an activated conduction mechanism. Typically, the first arc is related to the bulk contribution and the second one to the grain boundary contribution to conductivity.

Above 600 K, the Z^* plots consist of single semicircles with a nonzero intercept at high frequency. This value diminishes upon increasing the temperature, the non-zero intercept indicates the presence of an arc with ω_{max} higher than the maximum frequency measured, about 10^5 Hz. Therefore, the intercept at high frequencies could, in principle, be attributed to the bulk or grain resistance, R_1 [31], that is, temperature-dependent (see Fig. 7). Conductivity data are obtained from the corresponding resistance values at low frequencies and are plotted against reciprocal temperature in Arrhenius format in Figure 8. The activation energy value, E_a = 0.95(1) eV, is obtained by fitting the experimental log σ values in terms of an exponential law, that is typical of small polaron hopping processes. One slope was obtained suggesting that only a conduction mechanism takes place in this material.

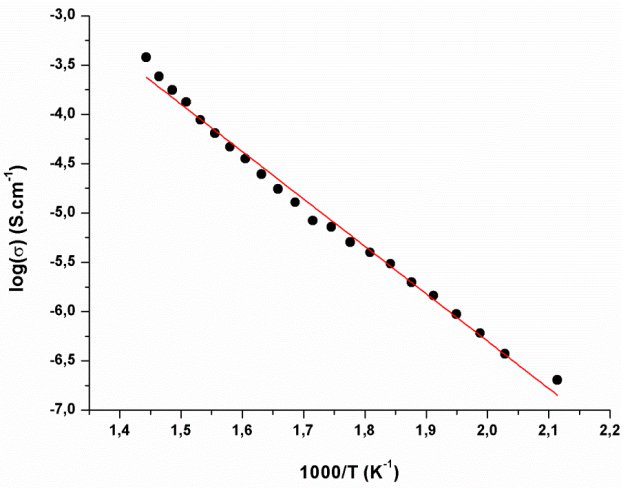

Figure 8: Conductivity variation vs 1000/T for $NaMnFe(MoO_4)_3$.

The E_a value is relatively high but comparable to other related compounds as shown in Table VI. The best sodium ionic conductors of this series are those of similar composition to the title compound, that is $NaMFe(MoO_4)_3$ (M = Ni, Zn)previously reported by us [14]. The observed variations in conductivity are due to differences in their structural characteristics. Indeed, in $NaMFe(MoO_4)_3$ (M = Ni, Zn), tunnels consist of large eight-membered rings of alternating MoO_4 tetrahedral and $[M,Fe]O_6$ octahedra, while in $NaMnFe(MoO_4)_3$ they are based on more narrow and complex rings. Furthermore, the jump distance from Na site to interstitial space (about 3.42 Å) along b axis in the Ni(Zn)-compounds, is shorter than 4.832 Å observed along [1 0 1] direction in the Mn-one.

The title compound, $NaMnFe(MoO_4)_3$ which adopts the α-$NaFe_2(MoO_4)_3$ structure, shows a conductivity value, around $1.1.10^{-8}$ S/cm at 573 K, lower than of $NaNiFe(MoO_4)_3$, $NaZnFe(MoO_4)_3$ and the NASICON-type conductors. However, this conductivity remains comparable to those of one-dimensional ion conductors, such as molybdates with Lyonsite-type structure. For comparison, $NaNiFe(MoO_4)_3$ and $NaZnFe(MoO_4)_3$ compounds which are isostructural with β-$NaFe_2(MoO_4)_3$, have at 500 K conductivities around $2x10^{-4}$ S/cm [14]. Along the series of NASICON type compounds with

Table VI: Chemical composition and ionic conductivity data for NASICON-type phosphates and one-dimensional ion conductor molybdates.

Composition	σ /S·cm^{-1} at T (K)	E_a/eV (Temperature range)	Ref.
$NaMnFe(MoO_4)_3$	$1.1x10^{-8}$ (573)	0.95 (473-513)	This work
$NaNiFe(MoO_4)_3$	$1.9x10^{-4}$ (523)	0.29 (293-473)	[14]
$NaZnFe(MoO_4)_3$	$2.7x10^{-4}$ (473)	0.36 (293-473)	
$NaZr_2(PO_4)_3$	$2.5x10^{-4}$ (573)	0.51 (373-573)	[32, 33]
$LiZr_2(PO_4)_3$	$5.0x10^{-4}$ (573)	0.28 (573-723)	[34]
$LiNbFe(PO_4)_3$	$6.6x10^{-6}$ (623)	0.85 (473-873)	[35]
$Li_3Fe(MoO_4)_3$	$6.6x10^{-7}$ (573)	1.11 (473-873)	[36]
$Li_2Mg_2(MoO_4)_3$	$1.1x10^{-7}$ (573)	0.71 (473-673)	
$Na_{2.2}Zn_{0.9}(MoO_4)_2$	$7.1x10^{-7}$ (573)	0.85 (473-673)	[37]
$Na_{1.92}Mg_{2.04}(MoO_4)_3$	$3.0.10^{-7}$ (683)	1.37 (673-773)	[38]

general formula $AMM'(PO_4)_3$, conductivity varies at 573 K from $6.6x10^{-6}$ S/cm for $LiNbFe(PO_4)_3$ to $2.5x10^{-4}$ and $5.0x10^{-4}$ S/cm for $NaZr_2(PO_4)_3$ and $LiZr_2(PO_4)_3$ respectively [32-35]. In the system $Li_{2+x}Mg_{2(1-x)}Fe_x(MoO_4)_3$ with Lyonsite-type structure conductivity ranges at 573 K from $1.1x10^{-7}$ for $Li_2Mg_2(MoO_4)_3$ (x = 0) to $6.6x10^{-7}$ S/cm for $Li_3Fe(MoO_4)_3$ (x = 1)[36].

CONCLUSION

$NaMnFe(MoO_4)_3$ has been prepared both as single crystals and powder form and characterized by X-ray diffraction, magnetic measurements and ionic conductivity. This compound is isostructural with α-$NaFe_2(MoO_4)_3$. Its structure exhibits an anionic three-dimensional framework built up from $[Mn,Fe]_2O_{10}$ bi-octahedra connected to each other through the MoO_4 tetrahedra. The resulting tunnels along the [1 0 1] direction can be considered as made up of Na_2O_{14} dimers alternating interstitial spaces. The magnetic susceptibility measurements show the title compounds antiferromagnetic with C_m = 9.03 emu K/mol and θ = -65.5 K. Ionic conductivity results confirm that this material is ionic conductor with activation energy: 0.95 eV comparable to those of one-dimensional ion conductors such as molybdates with Lyonsite-type structure. This, allows us to consider it as promising solid electrolyte. Additional work is required to clarify the role of the cationic substitution on the behavior of the observed ionic conductivity.

REFERENCES

[1] S. H. Tian, Y. T. Tu, D.S. Chen, X. Chen, Y. Xiong, *Chem.Eng.J.*, **2011,** 69, 31.
[2] A. M. Beale, S. D. M. Jacques, E. Sacaliuc-Parvalescu, M. G. O'Brien, P. Barnes, B. M. Weckhuysen, *Appl. Catal. A. Gen.*, **2009,** 363, 143.
[3] E. V. Sinyakov, E. F. Dudnik, T. M. Stolpakova, O. L. Orlov, *Ferroelectrics*, **1978,** 21, 579.
[4] M. Maczka, A. Pietraszko, G. D. Saraiva, A. G. Souza Filho, W. Paraguassu, V. Lemos, C. A. Perottoni, M.R. Gallas, P. T. C. Freire, P. E. Tomaszewski, F. E. A. Melo, J. Mendes Filho, J. Hanuza, *J. Phys. Condens. Matter.*, **2005,** 17, 6285.
[5] M. Maczka, M. Ptak, C. Luz-Lima, P. T. C. Freire, W. Paraguassu, S. Guerini, J. Hanuza, *J. Solid State Chem.*, **2011,** 184, 2812.
[6] M. Devi, U.V. Varadaraju, *Electrochem. Comm.*, **2012,** 18, 112.
[7] A. A. Savina, S. F. Solodovnikov, O. M. Basovich, Z. A. Solodovnikova, D. A. Belov, K. V. Pokholok, I. A. Gudkova, S. Yu. Stefanovich, B. I. Lazoryak, E. G. Khaikina, *J. Solid State Chem.*, **2013,** 205, 149
[8] R. F. Klevtsova, *Dokl. Akad. Nauk. SSSR*, **1975,** 221, 1322.
[9] E. Muessig, K. G. Bramnik, H. Ehrenberg, *Acta Cryst. B,* **2003,** 59, 611.
[10] H. Ehrenberg, E. Muessig, K. G. Bramnik, P. Kampe, T. Hansen, *Solid State Sci.*, **2006,** 8, 813.

[11] K. G. Bramnik, E. Muessig, H. Ehrenberg, *J. Solid State Chem.,* **2003,** 176, 192.
[12] I. Yu. Kotova, N. M. Kozhevnikova, *Russ. J. of App. Chem.,* **2003,** 76, no. 10, 1572.
[13] N. M. Kozhevnikova, A. V. Imekhenova, *Russ. J. of Inorg. Chem.*, **2009,** 54 (4), 638-643.
[14] M. Mhiri, A. Badri, M. L. Lopez, C. Pico, M. Ben Amara, *Ionics,* **2015,** 21, 2511.
[15] M. S. Michael, A. Fauzi, S. R. S. Prabaharan, *Inter. J. Inorg. Mater.,* **2000,** 2, 261.
[16] A. C. T. North, D. C. Phillips, F. S. Mathews, *Acta. Cryst. A*, **1968,** 24, 351.
[17] A. Altomare, G. Cascarano, C. Giacovazzo, A. Guagliardi, *J. Appl. Crystallogr.,* **1993,** 26, 343.
[18] G. M. Sheldrick, "SHELXL97", A Program for the Solution of the Crystal Structure, University of Göttingen, **1997**.
[19] R.D. Shannon, *Acta Cryst. A,* **1976,** 32, 751.
[20] L. J. Farrugia, "WinGX", *J. Appl. Crystallogr.,* **1999,** 32, 837.
[21] R. Hoppe, S. Voigt, H. Glaum, J. Kissel, H. P. Müller, K. Bernet, *Journal of the Less-Common Metals*, **1989,** 156, 105.
[22] M. Nespolo, G. Ferraris, G. Ivaldi, R. Hoppe, *Acta Cryst. B,* **2001,** 57, 652.
[23] A. Juhin, G. Morin, E. Elkaïm, D. J. Frost, M. Fialin, F. Juillot, G. Calas, *Am. Mineral.,* **2010,** 95, 59.
[24] S. C. Abrahams, *J. Chem. Phys., 1967,* 6, 2052.
[25] W. T. A. Harrison, A. K. Cheetham, *Acta Cryst. C,* **1989,** 45, 178.
[26] J. P. Smit, P. C. Stair, K. R. Poeppelmeier, *Chem. Eur. J.,* **2006,** 12, 5944.
[27] A. van der Lee, M. Beaurain, P. Armand, *Acta Cryst. C,* **2008,** 64, i1.
[28]C. Bouzidi, M. F. Zid, A. Driss, A. Souilem, *Acta Cryst.E,* **2014,** 70, i36.
[29] G. Donnay, R. Allmann, *Am. Mineral.,* **1970,** 55, 1003.
[30] E. Barsoukov, J. R. Macdonald, Impedance Spectroscopy Theory, Experiment and Applications, second ed., John Wiley & Sons, New Jersey, **2005**.
[31] D. C. Sinclair, T. B. Adams, F. D. Morrison, A. R. West, *Appl. Phys. Lett.,* **2002,** 80, 2153.
[32] J. P. Boilot, G. Colin, P.Colomban, *J. Solid State Chem.,* **1988,** 73, 160.
[33] C. Delmas, J. C. Viola, R. Olazcuaga, G. Le Flem, P. Hagenmuller, F. Cherkaoui, R.Brochu, *Mater. Res. Bull.,* **1981,** 16, 83.
[34] F. Sudreau, D. Petit, J. P. Boilot, *J. Solid State Chem.,* **1989,** 83, 78.
[35] V. Thangadurai, A. K. Shukla, J. Gopalakrishnan, *J. Mater.Chem.,* **1999,** 9, 739.
[36] L. Sebastian, Y. Piffard, A. K. Shukla, F. Taulelle, J. Gopalakrishna, *J. Mater.Chem.,* **2003,** 13, 1797.
[37] J. Grins, M. Nygren, Solid State Ion., **1983,** 9-10, 859.
[38] E. Ines, M. F. Zid, A. Driss, *J. Crystallogr.,* **2013,** 2013, 146567.